buildings

MDPI

Article

The Development and Performance of a Novel Switchable Shading Device

Etienne Magri [1,*], Vincent Buhagiar [1] and Mauro Overend [2]

[1] Department of Environmental Design, Faculty for the Built Environment, University of Malta, MSD 2080 Msida, Malta; vincent.buhagiar@um.edu.mt
[2] Department of Architectural Engineering & Technology, Faculty of Architecture & Built Environment, TU Delft, Building 8, Julianalaan 134, 2628 BL Delft, The Netherlands; m.overend@tudelft.nl
* Correspondence: etienne.magri.99@um.edu.mt

Abstract

Existing buildings with large glazing ratios within subtropical Mediterranean climates face substantial challenges for thermal and visual control of their indoor environment. Previous research by the same authors has already identified the potential of incorporating both solar–PDLC (polymer-dispersed liquid crystal) and SPD (suspended particle device) switchable films within facades exposed to high solar insolation to provide a wide dynamic range of visual transparencies. This paper identifies a novel application for switchable laminates within a dynamic external shading device that permits the casting of a shadow on demand onto existing fenestration. This study compares the degree of glare within an enclosed space attained by a conventional opaque overhang over a window to that achieved with glass shading overhangs incorporating two types of switchable films. Using a scale model in a field test setting, indoor illumination and glare measurements are investigated under different states of switchable films and compared to those provided by conventional static glazing, with and without ordinary external overhangs under identical field test conditions. Results show that switchable overhangs in their transparent/bleached state can allow the ingress of daylight without creating excessive glare, whereas in their translucent/tinted state, switchable shades can deliver a level of glare protection similar to that provided by an opaque shading overhang.

Keywords: switchable glazing; adaptive facades; dynamic external shading; glare; occupant well-being

Academic Editor: Marcin Brzezicki

Received: 11 February 2026
Revised: 28 March 2026
Accepted: 5 April 2026
Published: 13 April 2026

1. Introduction

1.1. Background

Design trends in office buildings, even in cooling-dominated climates such as that in the Mediterranean, continue to favour façades with high glazing ratios. While this approach helps create buildings that appear "modern and transparent", which can increase real estate value, it has also led to significant heating and cooling demands [1]. Although research continues to improve building fabric properties for reducing energy consumption, substantial studies have focused on how to enhance occupant comfort, particularly in terms of indoor visual environment quality [2]. The importance of a comfortable, glare-free indoor visual environment can never be underestimated. Internal shading devices, such as window blinds, are often used as quick and inexpensive solutions to modify (to a certain extent) the quality of daylighting. While these devices help control glare, they often obstruct

views and increase the need for artificial indoor lighting, while largely failing to effectively address the overheating issue. External shading devices such as overhangs are known to perform better at reducing unwanted solar heat gain, but when completely static, they lack seasonal and diurnal adaptability that building occupants often demand. Although external dynamic shading is possible, the required moving components exposed to external environmental conditions are susceptible to breakdown and would require significant maintenance. The development of an adaptable, solid-state shading device would thus help to resolve these issues.

1.2. External Shading and Adaptive Glazing

Glare is a "negative sensation" caused by "bright areas with sufficiently greater luminance that the luminance to which the eyes are adapted to, producing annoyance, discomfort or loss in visual performance and visibility" [3]. This standard emphasizes the importance of shielding building occupants from glare with shading devices to reduce exposure from direct sunlight.

Passive external shading overhangs on windows have long been in use and offer several benefits, especially in terms of energy efficiency and occupant comfort. Opaque overhangs shield the indoor environment from direct solar radiation and sky-component radiation, which helps prevent excessive heat from entering the indoor space as well as reducing the surface temperature of glazed areas. This is particularly effective in warm climates. By reducing solar heat gain, overhangs reduce the need for air conditioning, thereby lowering energy consumption and cooling costs. They also help maintain a more consistent indoor temperature, making the interior more comfortable throughout the day and year-round by reducing discomfort from thermal asymmetry. Overhangs also prevent direct views of the sun, which reduces glare, providing a more pleasant indoor environment; they can also help balance the amount of natural light entering the space without compromising visual comfort. With proper design, overhangs can allow diffused light into the interior, enhancing natural light quality without the harshness of direct sunlight. One drawback of fixed external shading devices is their lack of adaptability and occupant control. Their effectiveness often depends on their appropriate design in relation to the seasonal position of the sun, with horizontal overhangs effective on southern facades. However, shades oriented vertically are more effective on eastern and western-facing facades.

Switchable glazing, on the other hand, may be one of the most promising technologies for solar control mechanisms available on the market. Smart glazing is a type of glass that can modify the radiative energy transfer (visible light transmittance and g-values) of a glazing system, while the conductive heat transfer (U-value) remains mostly unaffected. Dynamic glazing technologies are divided into 'passive' and 'active' types, with the active ones achieving optical and thermal property adjustment by voltage or electric current. Electrically controllable dynamic glazing technologies include electrochromic glazing (EC); suspended particle devices (SPDs); and liquid crystal devices (LCs) among other technologies. SPDs and polymer-dispersed liquid crystal devices (PDLCs) are two separate promising technologies already in use in the automotive and aviation sectors that already offer an excellent level of glare control and privacy in vehicles and aircraft. Similarly, potential exists in buildings wherein occupants spend a much greater amount of time, and the use of these technologies in windows creates new possibilities for the adaptability of the building envelope. Besides the control of glare, the capability of PDLC materials to ensure privacy adds value to a façade, allowing it to fully isolate its occupants from the outside, particularly after sunset. The importance of privacy is well recognized in psychological

research, described as the need for individuals or groups of people to control their visual, acoustic, and olfactory interactions within the built environment and with others [4].

1.3. The Concept of a Novel Switchable Shade

By definition, a PDLC (polymer-dispersed liquid crystal) film can be applied either as a self-adhesive plastic film onto existing glass or laminated onto glass-end products, such as 'smart windows'. This technology provides privacy, security, and ultimately energy efficiency. The technology is electronically switchable and can be turned ON (transparent) or OFF (translucent), with some manufacturers offering intermediate translucence states. Separately, an SPD (suspended particle device) film allows glass to change from a fully bleached (switched ON) to a fully tinted state (switched OFF) and can even be dimmed to any state in between. SPD technology can restrict up to 99% of visible light for high-performance glazing and is intended to replace traditional shading blinds or complex mechanised indoor blinds.

Solar–PDLC and SPD switchable technologies have clearly distinctive properties: privacy and dispersion of incident solar radiation and the ability to control the levels of daylight to potentially achieve a glare-free indoor environment. Previous research has already identified the potential of deploying both solar–PDLC and SPD switchable films within facades exposed to high solar insolation to provide a wide dynamic range of visual transparencies [5]. Moreover, both technologies appear to have one common property, i.e., that of being able to cast a shadow in their OFF state (translucent in the case of the solar PDLCs and tinted in the case of the SPDs). This specific property is thought to unlock a possible new application for the use of these films, particularly that of being embedded within a glazing laminate such that when installed horizontally as a fixed, external overhang, it will result in an adaptive switchable shading device. An illustration of this concept is shown in Figure 1.

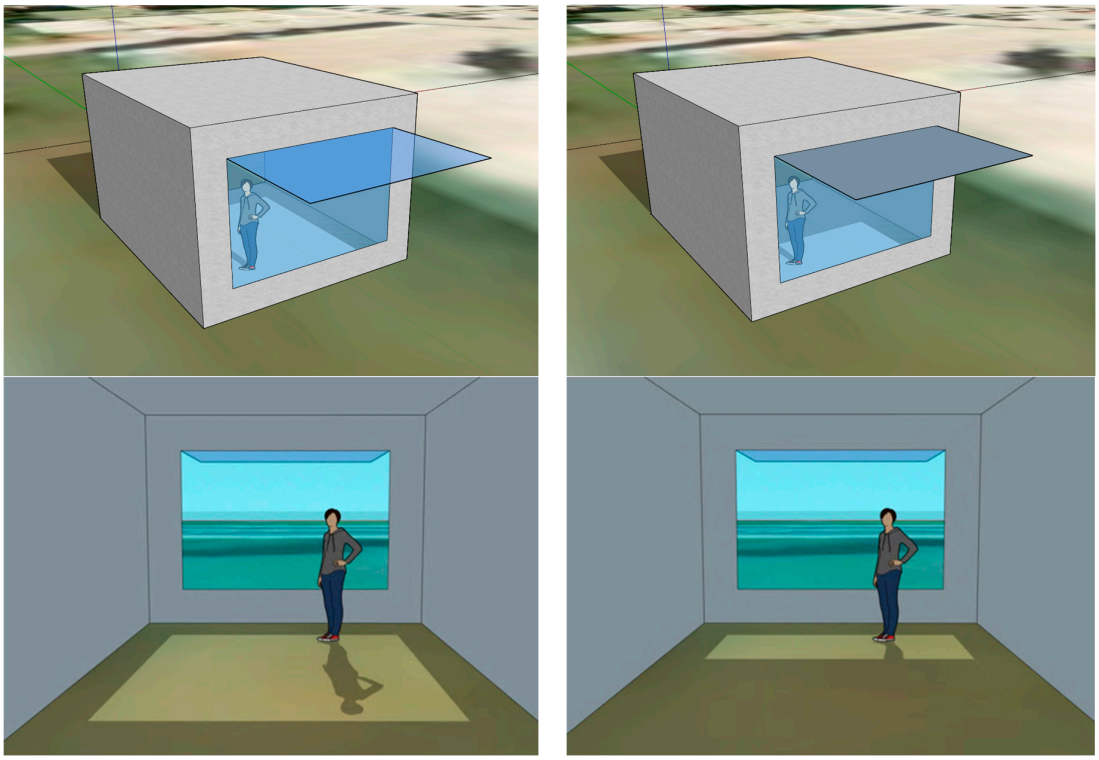

Figure 1. Conceptual representation of the deployment of switchable glazing as an external shading overhang.

1.4. Scale Model Testing

The objective of this study is to investigate the potential of switchable films to be deployed within a more conventional building element, in this case a shading overhang, equally suitable for retrofitting of existing facades. A thorough assessment of the visual and thermal performance of such innovative elements would be required by means of a full-scale field study, assessing long-term visual and energy performance, conducting on-site monitoring experiments, as well as collecting responses from human subjects. As a prelude to this, a 1:10 scale model of an office space was used for a preliminary field assessment of the visual performance of two switchable glazing technologies for comparison to industry-grade static glass with solar control coatings and a conventional opaque shading overhang. The two principal objectives of these field tests were as follows:

1. To measure the indoor lighting conditions within a scale model fitted with three static glass samples with different visible light transmittances and with and without an overhang fitted above the window.
2. To assess the potential of having two distinct switchable glass overhangs installed on a south-facing façade, eventually in a full-scale setup, giving the building occupant the freedom to instantly deploy (or not) the effect of a shading overhang.

Scale models under field test conditions for the analysis of visual and thermal properties of switchable glass have been adopted in other studies, primarily by Ghosh and Norton in their studies of glazing samples with SPD [6–8]. In their research, tangible results were reported for the various metrics collected in their experiments, including the Daylight Factor (DF), Daylight Glare Index (DGI) and Useful Daylight Illuminance (UDI). Bodart & Cauwerts [9] and Yngvesson & Adolfsson [10] concluded that the quality and quantity of light in scale models are identical to those present in real conditions if material properties are respected in the construction of the scale model and if the environmental conditions are identical for both full-scale and scale model experiments. Specifically, the conclusions drawn by Yngvesson & Adolfsson state that a 1:10 scale model setup is the most representative of real room conditions when compared to 1:20 and 1:50 scale models, due to the latter being too small for the perception of the shape and detail of the interior of the room.

1.5. Metrics for the Measurement of Glare

This paper looks at the level of glare achieved within an indoor space when subjected to a switchable shade deployed as an overhang over a window fitted with conventional static glass. To achieve this, this work investigates a series of field test experiments intended to physically test the visual performance achieved by the "switchable shading property" of smart glazing and its effect on the indoor visual environment without obstructing outward views. The quality of an indoor daylit environment can be measured using various metrics. The Daylight Factor (DF) is the ratio of the indoor illuminance at a point in a room to the outdoor illuminance under overcast sky conditions, usually expressed as a percentage, whereas Lighting Uniformity measures how evenly light is distributed across a space and is calculated by dividing the minimum illuminance by the maximum illuminance. Since the presence of glare is often considered a primary cause of discomfort, especially in offices featuring a high glazing ratio, the appropriate measurement of this quantity is considered a key parameter for a preliminary assessment of the performance of these switchable shades in this study. Other factors such as Lighting Uniformity and illuminance levels further contribute to the comfort and functionality of an interior space.

Various glare indices have been developed over the years. In 1972, Hopkinson first attempted to quantify glare from daylight through the establishment of the "Daylight Glare Index" (DGI), which "had the merit to introduce in its equation all the main factors

potentially concurring in the determination of a glare condition from daylight: luminance and solid angle of the light source, average luminance of the background, position of the light source relative to the observer's field of view" [11]. Iwata and Waters [12–14], however, show that "DGI showed a low reliability as a glare predictor in presence of windows, especially when these occupy most of the observer's field of view, or when the sun is in the occupant's visual field". Velds [15] later simplified the calculation of daylight glare and attempted "to estimate it by using the vertical illuminance at the observer's eyes, in replacement of the background luminance". The most reliable metric for measuring glare in an indoor space is the Daylight Glare Probability (DGP). This metric is widely used because it considers both the intensity and the spatial distribution of daylight in the space, offering a comprehensive assessment of glare based on human visual perception. In 2006, Wienold and Christoffersen [16] introduced this new metric for the computation of glare, expressing "the percentage of occupants disturbed by a daylighting glare situation". Compared to traditional indices such as DGI or UGR, the DGP method offers superior accuracy in daylit environments by integrating vertical eye illuminance into the glare calculation. This metric is particularly suited for evaluating the comparative field test approach analysed in this study, aligning the current work with established international standards and recent advancements in occupant-centric building performance studies [17].

2. Materials and Methods

2.1. Methodology

This study utilizes a comparative experimental research design to evaluate the glare reduction potential of switchable glazing when integrated into external shading devices. The methodological framework is grounded in quantitative empirical analysis, using physical scale modelling (1:10) to simulate complex daylighting phenomena. This approach allows for a validated assessment of luminance distribution and visual comfort, as measured by the Wienold Daylight Glare Probability (DGP) metric. By translating raw physical luminance data into a statistically significant measure of occupant visual comfort, the findings are thus aligned with current international standards for indoor environmental quality (IEQ).

The study is structured around a controlled-variable analysis, where the performance of the switchable shading device under investigation is benchmarked against two distinct controls:

1. Baseline (Unshaded): An open-aperture scenario to establish maximum glare risks;
2. Static Control: An opaque matte white overhang representing a conventional architectural shading device that is geometrically identical to the switchable glazing overhangs.

By maintaining identical geometries between the test and control groups and utilizing a temporal control window (60 min) to ensure stable sky conditions, this design isolates the "switching state" of the glazing as the primary independent variable. This ensures that observed variations in DGP are directly attributable to the optical properties of the shading material rather than environmental or geometric flux.

The assessment of visual discomfort in this study is conducted using the Daylight Glare Probability (DGP) metric, which quantifies the probability that a person is disturbed by daylight glare. The DGP is calculated by integrating vertical eye illuminance with the luminance, solid angle, and position of glare sources within the occupant's field of view, as expressed in Equation (1):

$$DGP = 5.87 \cdot 10^{-5} \cdot E_v + 9.18 \cdot 10^{-2} \cdot log\left(1 + \sum_i \frac{L_{s,i}^2 \cdot \omega_{s,i}}{E_v^{1.87} \cdot p_i^2}\right) + 0.16 \quad (1)$$

where $L_{s,i}$ is the source luminance (cd/m^2), $\omega_{s,i}$ is the solid angle, E_v is the vertical illuminance (lux), and p_i is the Guth position index for the field of view". DGP is mainly influenced by the first term (E_v) with the second term relating to the apparent contrast. This method for the assessment of glare now forms part of EN 17037:2018 [4] and is widely considered the standard approach for the computation of glare. Pierson et al. describe a methodology for the computation of point-in-time glare through the generation of luminance maps from high-dynamic-range photography and using semi-professional equipment while further describing analytical methods for the simulation of glare using Evalglare software [18,19].

The classification of glare has previously been based on the four-point scale described by Wienold [16,20] and adopted in similar studies, such as that by Reinhard and Wienold [21], wherein glare discomfort is classified into classes: imperceptible glare (DGP < 35%); perceptible glare (35% $\leq$ DGP < 40%); disturbing glare (40% $\leq$ DGP < 45%) and intolerable glare (DGP $\geq$ 45%). A graphical representation of this four-point scale is shown in Figure 2. Thanks to this seminal research, this categorization now also forms an integral part of the normative standard EN 17037:2018.

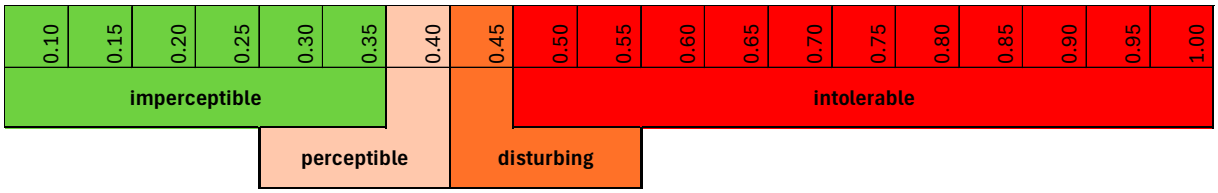

Figure 2. Graphical representation of the DGP four-point scale classification [16].

Due consideration was given to the potential effect of using a scale model for field testing and the computation of the DGP from the luminance maps generated by the luminance photometer. The DGP formula is dependent on four variables, all of which are theoretically scale independent. Vertical illuminance (E_v) is the density of luminous flux. If the light source (the sun in this case) remains constant, the amount of light hitting a point in a model is the same as that in real world, regardless of the room's size. Luminance $\left(L_{s,i}\right)$ is "brightness" per unit area, which is inherently scale independent. For instance, a white wall under 500 lux has the same luminance (cd/m^2) whether it is 10 metres wide or 1 metre wide. The solid angle ($\omega_{s,i}$) is the "size" of the glare source in the field of view. The solid angle remains constant, since it is defined by the ratio of a source's area to the square of its distance from the observer ($\Omega = \frac{A}{r^2}$). When a setup is scaled down, for instance by a scale of 10, distances decrease by that factor, but the surface area of the light source decreases by that factor squared. Because both the numerator (area) and the denominator (distance squared) shrink by the exact same proportion, they cancel each other out perfectly. This ensures the geometric "view" remains identical, whether one is looking at a full-sized room or a 1:10 model. The position index (p_i) is based on the angular displacement from the line of sight, and angles do not change with scale. This therefore explains why the scale factor for luminance photometer measurements taken within a scale model (1:10) cancels out for each variable.

Practical considerations for the use of the 1:10 model were also carefully considered. The placement of the luminance photometer was chosen to ensure that no self-shading was experienced within the model itself. Moreover, to avoid errors related to the precision of placement of instrument, utmost care was taken to ensure that both the luminance photometer and the scale model itself were secured at the same identical positions across the tests when replacing the façade glass samples and the different types of shading overhangs. Cognisant of the fact that the surface reflectance and texture of the model's materials might

appear slightly more specular than the same material at full scale, this experiment sought to relatively compare DGP values provided by different shading overhangs in different switching states while using the same unaltered scale model across the experiments.

For the scope of this study, readings for the parallel light transmittance of each of the samples were taken by a calibrated WTM-1200 tint meter, with resolution of 0.1 and an accuracy of ≤2%. The primary objective of the field test was the generation of a dataset of luminance images taken under identical climatic considerations for the subsequent analysis of glare as perceived by the human eye. To achieve this, a series of high-resolution images were taken at different exposure times using the TechnoTeam® LMK Mobile-R (TechnoTeam Bildverarbeitung GmbH, Ilmenau, Germany)image-resolved luminance photo camera for field measurements, equipped with a SIGMA 4.5 mm 1:2.8 circular fish-eye lens. Following the generation of a high-dynamic-range [HDR] photograph for each scene, luminance maps were created using the TechnoTeam® proprietary LMK LabSoft 14.3.6® suite. Apart from the identification of all light sources in the field of view of the observer, the Daylight Glare Probability [DGP], as described by Wienold and Christoffersen [15], was computed through software, this metric giving a reliable indication of the potential discomfort or otherwise to the observer when facing the window from a seated position. The luminance camera used in this study was designed specifically for such research use and thus was already calibrated by the manufacturer with detailed data sets and corrections for response curves, vignetting, and point source errors, directly embedded in Labsoft 14.3.6® software. This provided accurate luminance readings not requiring any further calibration. Thus, the software was able to handle the entire procedure of merging all photos into a single HDR, the creation of the luminance map, and calculating the DGP.

Two pilot test runs were carried out on 28 January under a clear sunny sky and on 26 February under a partly cloudy sky to assess the suitability of testing rig used for this study. For these preliminary tests, all the interior surfaces of the scale model were kept white in colour. Conscious of the fact that white flooring may not be representative of a typical indoor space, a light brown colour was chosen for the model's flooring prior to conducting the 1 March experiment, the results of which have been included in this paper. Moreover, the consistent clear sky conditions on 1 March provided for more uniform external daylighting conditions. All photos were taken facing south between 11:30 am and 12:30 am, with the sun in its highest position in the sky, in order to minimize effects of transient weather and sky conditions that could have had a bearing on the results. Facing south on 1 March, the solar angle of elevation at midday in Malta (35°54′5″ N 14°28′79″ E) was approximately 47° and allowed for the formation of a solar patch occupying an area of approximately 28% of the floor area of the space, considering a window 2.9 m wide by 2 m high (Figure 3). This orientation and the time window for testing were chosen to capture the worst-case scenario of a solar patch within the central zone of the field of view. The area thus illuminated by the solar patch could potentially have a perception of glare to an occupant. With a shading overhang projecting 2.4 m from the facade, no solar patch was formed, thus allowing this experiment to investigate the effect of switchable overhangs on the perception of glare.

The luminance camera was positioned at 40 cm from the glazed opening within the model, representing an occupant in a seated position at a distance of 4 m from the glazed façade. The camera was mounted on a secure base, with a series of 5 photographic shots each taken at different exposure times [1/250 s, 1/200 s, 1/160 s, 1/125 s and 1/100 s] to create an HDR image for the eventual processing through software. The images collected were analysed using the LMK Labsoft® software suite, wherein a series of high-dynamic-range images were first created for each scene, followed by the generation of a dataset of high-resolution luminance images. For the analysis of glare, the threshold

luminance for each scene was set at 3000 cd/m^2, corresponding to the threshold for visual discomfort as suggested by Bian and Luo [22]. This value of 3000 cd/m^2. is midway within a range specified by Wienold and Christofferson [23], with luminance values < 1500 cd/m^2 likely to be perceptible and >4500 cd/m^2 likely to be uncomfortable for a view direction perpendicular to a window. In all cases, the solar disc was never in the direct field of view. This ensured that none of the pixels within the luminance maps would experience luminous overflow, thus increasing the accuracy of the results obtained.

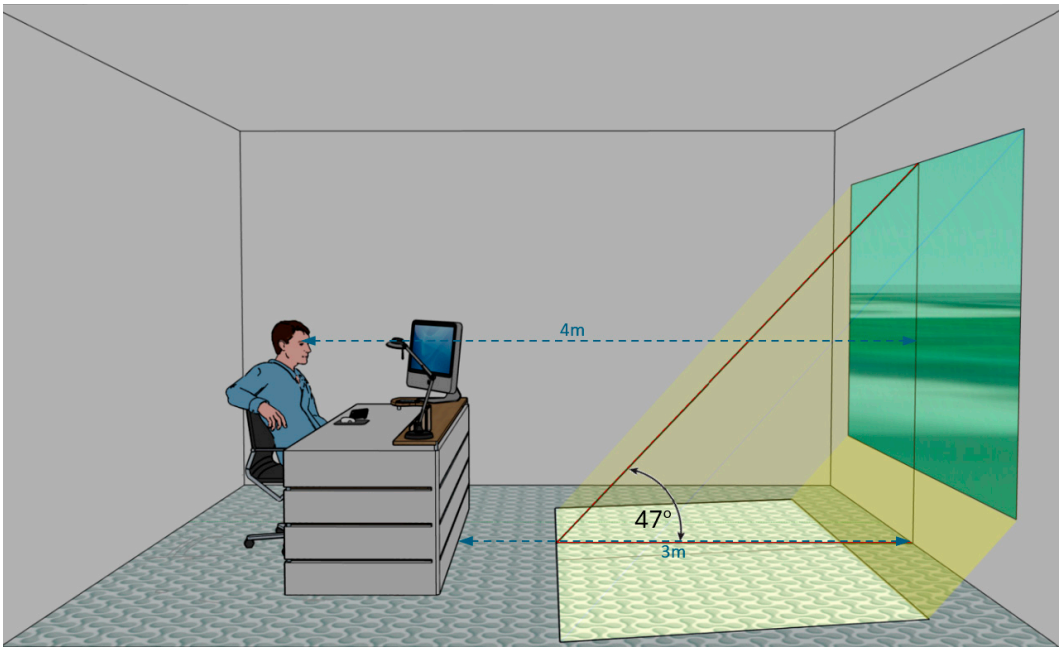

Figure 3. Representation of the simulated observation position in relation to the size of the solar patch on 1 March at 11:30 am with a solar altitude angle of 47°.

2.2. Experimental Setup

2.2.1. Scale Model Assembly

Making use of a sample set of static and switchable glazing samples of dimensions 290 × 200 mm as provided by the switchable film manufacturer and considering the appropriateness on the use of a scale model to collect preliminary data, a physical model of a room scaled 1 in 10 was assembled as shown in Figures 4 and 5, having an indoor dimension of 400 mm in width; 500 mm in depth; and 260 mm in height. The size of the scale model provided a glazing ratio of 56%, whereas due consideration was given to allow for the placement of a luminance photometer within the test box.

Attention was given to both the choice of materials and the assembly method to prevent any stray light or reflections to penetrate the scaled indoor space, other than that entering through the glazed aperture. Similarly, due consideration was given to ensure that the size of the scale model was large enough to capture the images in sharp focus. Thus, the luminance maps generated would have a similar geometrical appearance as those normally captured in a full-scale setup. For the scope of this experiment, the luminance photometer was positioned at one point of observation, directly facing the aperture, simulating a seated person facing the window. Although this position may not fully represent a typical seating arrangement in a room, this point of observation was deemed appropriate for this study as it represents a worst-case situation with the solar patch projected on the floor being directly in the field of view of the occupant. Notwithstanding this, comparing DGP readings for different switchable glazing configurations relative to static glass samples still provides a valid indication of which setup of switchable overhangs would potentially perform

best. Although scale factors could influence results in absolute terms when using scale models, it is assumed that in these experiments, the manner in which light enters the space is unaffected by the size of the testing chamber. Given the extremely small size of light wavelengths (380–790 nm), the physical behaviour of light remains unchanged in both full-size rooms and their scale models [24]. Since all measurements were taken under identical conditions for relative comparison, such factors should not affect the results.

Figure 4. External and internal views of the scale model used for the luminance field experiments, prior to the placement of the light brown flooring.

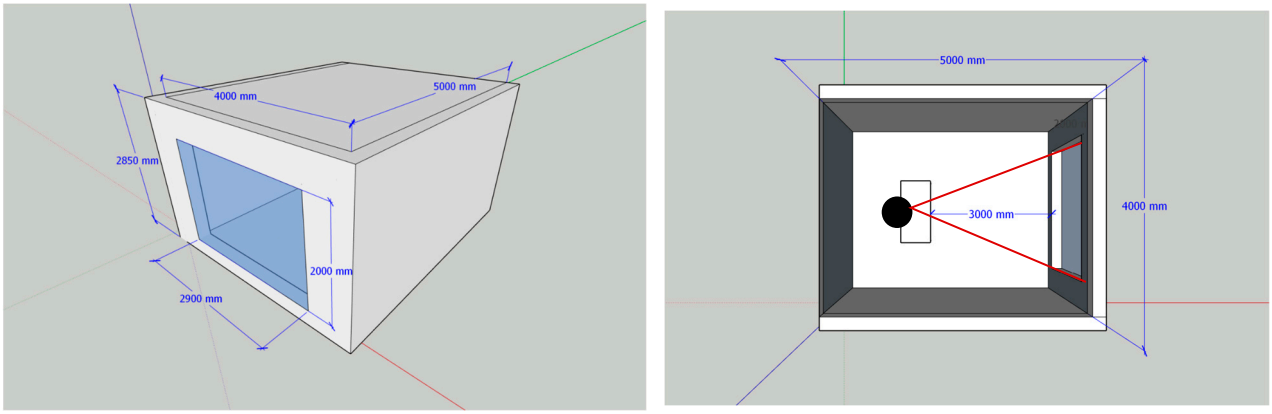

Figure 5. Three-dimensional graphic and plan of the simulated real-life office showing the assumed seated location and facing direction of an office worker.

2.2.2. Selection of the Glass Samples

Market research was conducted in collaboration with an established architectural glazing supplier in Malta to identify the most commonly ordered glazing products for use in curtain walls. The aim of this study was to select and test the performance of two types of switchable shades under field test conditions when installed as overhangs on three representative samples of static glazing. Three static glass samples were chosen with a visible light transmittance between 20 and 48% VLT, with their characteristics outlined in Table 1 and illustrated in Figure 6. The parallel light transmittance of each sample was measured using a calibrated WTM-1200 tint meter (Guangzhou Landtek Instruments Co., Ltd., Guangzhou, Guangdong, China) with a resolution of 0.1 and an accuracy of $\leq$2%.

Table 1. Technical characteristics of static glazing samples featuring a solar control coating.

Specimen ID	Brand Name	Configuration	Thickness [mm]	Visible Light Transmittance [%]
S1	Guardian SunGuard Solar Bronze 20 (Częstochowa, Poland)	Single-glazed unit	6	20
S2	Guardian SunGuard HP Bronze 40/27	Insulated glazed unit	6—10—4	40
S3	Saint Gobain KN148 (Dąbrowa Górnicza, Poland)	Single-glazed unit	8	48

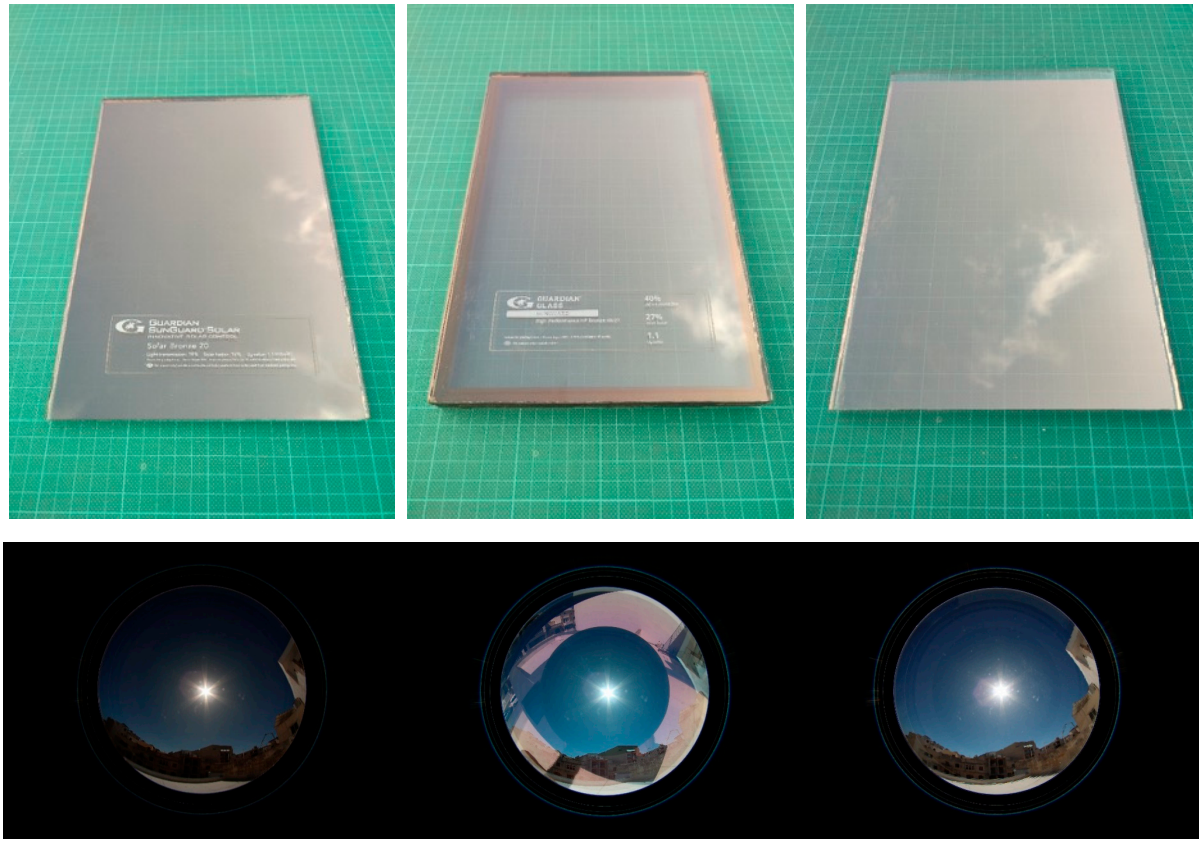

Guardian SunGuard Solar Bronze 20 | Guardian SunGuard HP Bronze 40/27 | Saint Gobain KN148

Figure 6. Photos of the static glazing samples featuring a solar control coating (**top**) and their appearance when placed perpendicular to the solar disc (**bottom**).

Two different configurations for the switchable shades were identified for testing a solar–PDLC (polymer-dispersed liquid crystal) laminate and an SPD (suspended particle device) laminate. The build-up of these laminates comprised the following:

- Switchable solar–PDLC film laminate [4 mm clear glass + EVA interlayer + PDLC film + EVA interlayer + 4 mm clear glass]
- Dimmable SPD film laminate [4 mm clear glass + EVA interlayer + SPD film + EVA interlayer + 4 mm clear glass]

The technical characteristics of these switchable shades are as featured in Table 2 and the appearance of the solar disc when viewed through each of the shades in their different switching states, as shown in Figure 7.

Table 2. Technical characteristics of the switchable shades under consideration.

Specimen ID	Configuration	Switching State	Thickness [mm]	Switching Time [s]	Parallel Light Transmittance * [%]
D1a D1b	Gauzy Solar-PDLC laminate (Gauzy Ltd., Tel-Aviv, Israel)	OFF (translucent) ON (transparent)	9.62	1	1 72
D2a D2b	Gauzy-Hitachi SPD laminate	OFF (tinted) ON (bleached)	9.79	3	0 45

Note. * Parallel light transmittance measured using a calibrated WTM-1200 tint meter with a resolution of 0.1 and an accuracy of ≤2%.

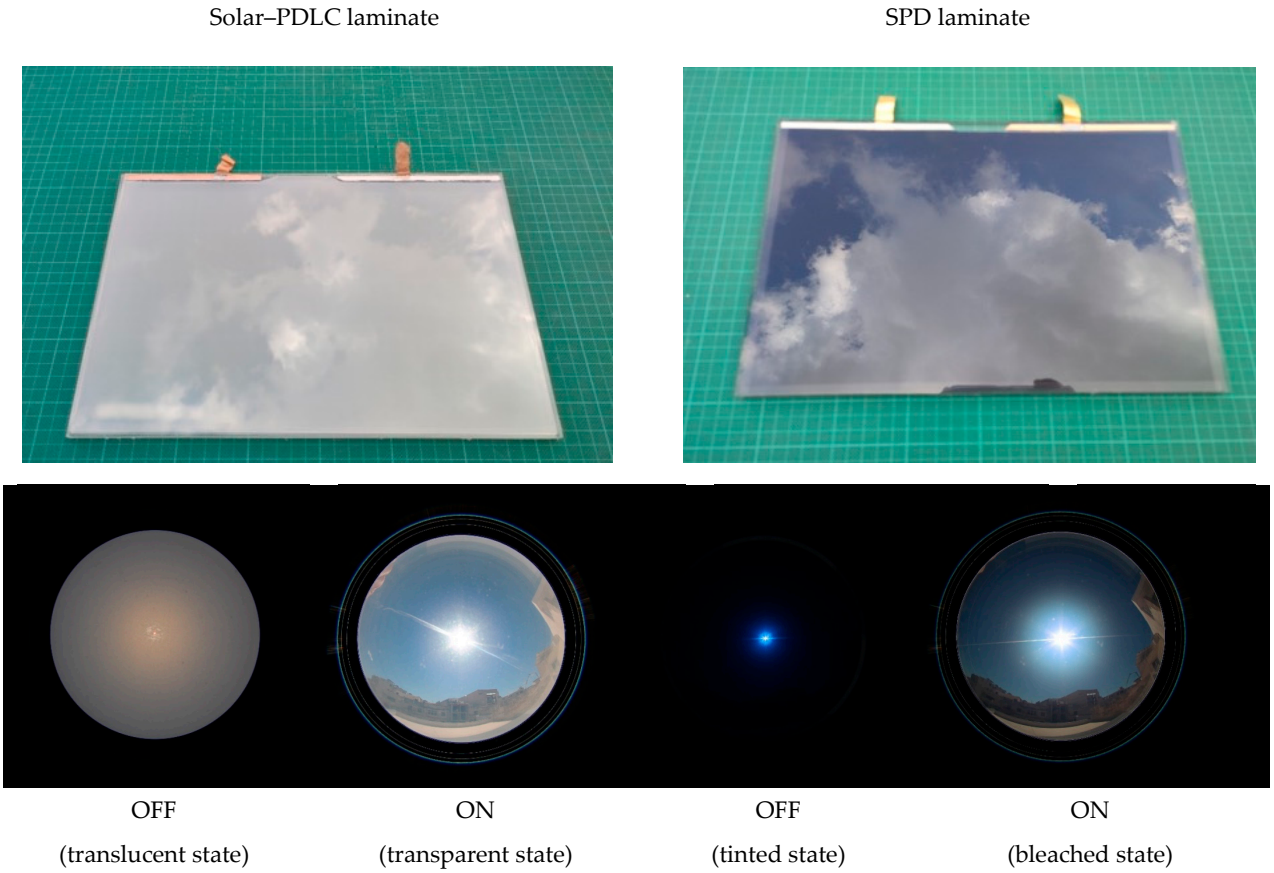

Figure 7. Photos of the switchable glazing samples for deployment as overhangs (**top**) and their appearance when placed in front of the solar disc (**bottom**).

2.2.3. Testing Setup

The setup required for testing primarily included the identification of a south-facing location free from shadows and obstructions to capture a set of high-resolution images from within the test box itself. For this purpose, the roof of a building in a built-up area was chosen as the testing location, providing a long-distance view of a sky area within the upper-third of the view through the model's window. The test box was mounted on a secure support to permit the interchanging of glass samples and overhangs as required, without any movement to the overall setup. The static glass samples acting as the window for the model was mounted on the model to prevent any stray light from entering the test box other than through the glass itself. The switchable glass overhangs were mounted onto a metal sub-frame cantilevered from the test box itself, which supported the weight of the glass while allowing for the necessary wiring to the electronic controllers. Neither the support nor the wiring cast undesirable shadows into the test box that would affect the images captured. The interior of the test box was kept entirely white for one of the test

runs, whereas for two of the three tests, a light-brown coloured sheet of cardboard was placed at the bottom to represent a darker flooring, typical of a real-world setup (Figure 8).

Figure 8. Selected photos of the testing setup. (**a**) Test box mounting on a secure base. (**b**) Luminance photometer within the test box. (**c**) Static opaque shading. (**d**) Unshaded configuration. (**e**) Solar–PDLC shading overhang (OFF state). (**f**) SPD shading overhang (OFF state).

To simulate an opaque shading overhang, a white sheet of foamboard was used, being completely opaque to the transmission of light; however, to prevent stray lighting from entering the model from the back end, an opaque blackout fabric was installed, with attention given to keeping the fabric in a secure position when images were shot.

Following the setting up of the testing rig, a preliminary visual assessment of this concept of "switchable shade" was conducted. An opaque cardboard tape dispenser tube was placed directly on top of the solar–PDLC switchable shade. In both ON and OFF states of the shade, two photos of the model's interior were taken as shown in Figure 9c,d. Toggling between the shade's ON and OFF states, the solar patch could be "switched" ON or OFF, effecting the visual condition of the interior lighting environment within the model. It could also be observed that the nature of the solar patch provided by the shade in its ON position appeared to have less visual contrast than the unshaded equivalent provided without any shading device, a property that was observed as having the potential for providing for a more soothing indoor lighting environment.

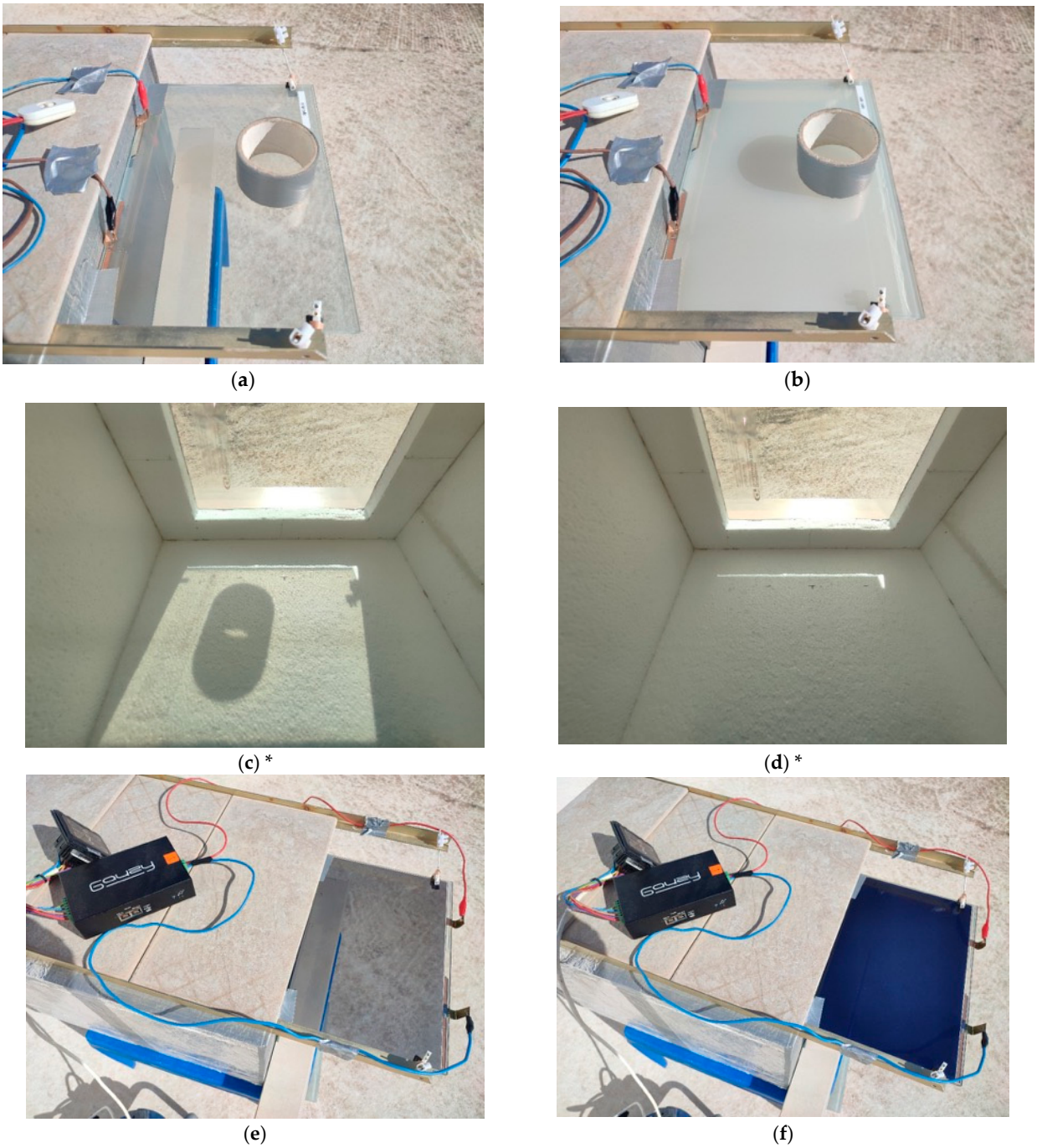

Figure 9. Preliminary visual assessment of the effect of solar–PDLC and SPD switchable shades. (**a**) Switchable PDLC shade _ON (transparent) state. (**b**) Switchable PDLC shade _OFF (translucent)

state. (**c**) Indoor effect with switchable shade in its ON state. Solar patch visible on the model's floor. (**d**) Indoor effect with switchable shade in its OFF state. No solar patch visible on the model's floor. (**e**) Switchable SPD shade _ON (tinted) state. (**f**) Switchable SPD shade _OFF (tinted) state. * Photo taken during the January pilot study prior to the installation of the brown-coloured flooring.

3. Results

A graphical representation of all luminance maps and the ranges of luminous intensity in cd/m^2 for each experiment is featured in this section. Results show the computed Daylight Glare Probability [DGP] and the number of light sources picked up by the luminance photometer based on the selected luminance threshold, as shown in the respective tables.

The results from tests carried out on 1 March 2025 are featured together with the respective luminance maps, from which the DGP values were computed. These values have been tabulated, expressed in histograms and observations noted. The three static glass samples have been tested for the computation of the DGP values attained within the scale model in various configurations, namely unshaded, shaded with an opaque overhang, shaded with a switchable PDLC overhang (ON and OFF states), and shaded with an SPD overhang (tinted and bleached states.)

3.1. Guardian Solar Bronze 20

Results obtained for the Guardian Solar Bronze 20 static glass sample are as shown in Table 3 and Figures 10 and 11. The values of the DGP of the six shading configurations tested all show values within the imperceptible range of the DGP four-point scale, confirming the effect of a very low VLT on the measurement of glare. Shading configuration S1 (unshaded) resulted in a much lesser value of the DGP (34.17%) than the other static glass samples, whereas in configuration S2 (shaded with opaque overhang), the measured DGP (21.48%) was not that much lower than those measured with other samples. Comparing these benchmark readings to those achieved with the subsequent four shading configurations (S3–S6), one can observe that the PDLC overhang in its transparent state allows for a reduction in the glare value to 29.01%, which is lower than the unshaded configuration. However, in its OFF (translucent) state, the DGP falls to 25.88%, again higher than that obtained with a fully opaque shading overhang. The SPD in its bleached state allows for a substantial reduction in the glare value to 22.8%, whereas in its OFF (tinted) state, the DGP attained (20.8%) results of a slightly lower value than that obtained with the opaque shading overhang. This latter result is likely due to the white colour of the opaque overhang, allowing for greater light reflections into the indoor space.

Table 3. Tabulated Results of the Guardian Solar Bronze 20 static glass sample.

Test ID [Shading State]	Configuration	DGP [%]	DGP Classification	Number of Light Sources Identified	Luminance Threshold [cd/m^2]
S1	Unshaded	34.17	imperceptible	56	3000
S2	Shaded (Opaque Overhang)	21.48	imperceptible	2	3000
S3	PDLC overhang ON (transparent)	29.01	imperceptible	4	3000
S4	PDLC overhang OFF (translucent)	25.88	imperceptible	3	3000
S5	SPD overhang ON (bleached)	22.80	imperceptible	2	3000
S6	SPD overhang OFF (tinted)	20.80	imperceptible	2	3000

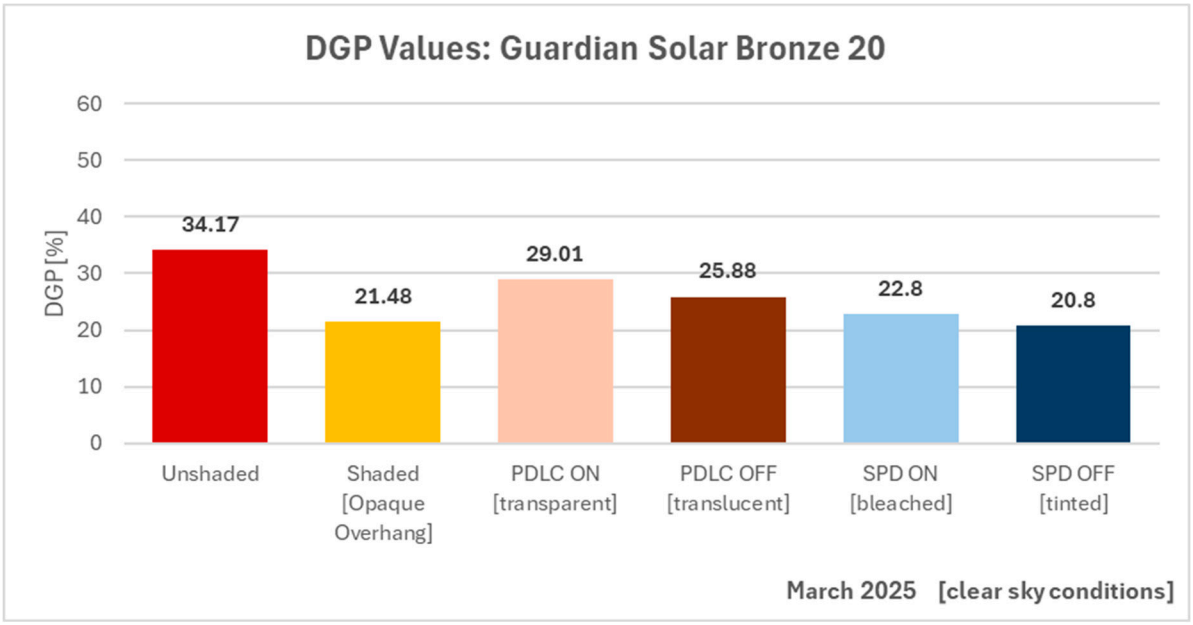

Figure 10. Graphical representation of the results of the Guardian Solar Bronze 20 static glass sample.

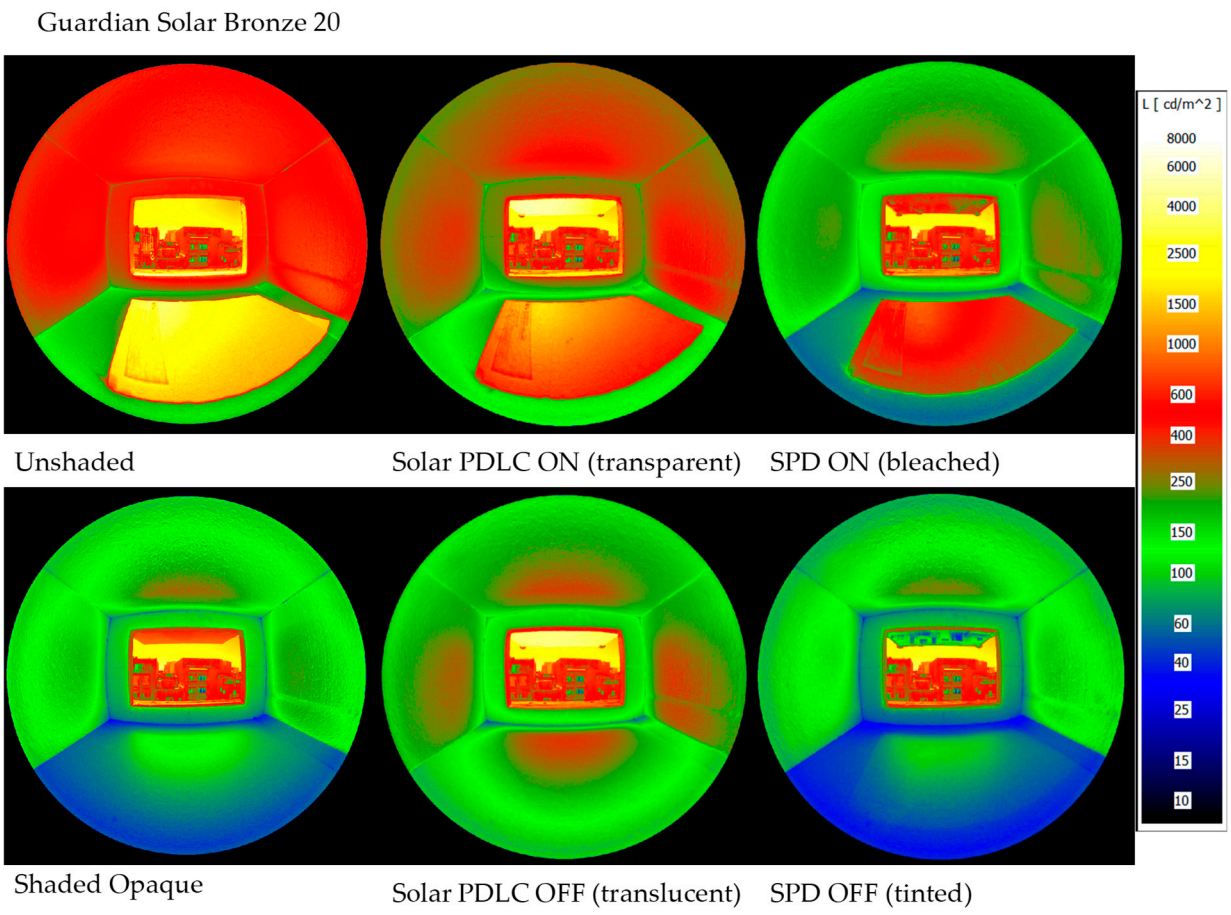

Figure 11. Luminance maps for the Guardian Solar Bronze 20 under different shading configurations.

3.2. Guardian SunGuard HP Bronze 40/27 IGU

Results obtained for the Guardian SunGuard HP Bronze 40/27 IGU static glass sample are as shown in Table 4 and Figures 12 and 13. The values of the DGP of the six shading configurations tested appear to correlate with the visible light transmittance of the sample under test and are generally slightly lower than the Saint Gobain KN148, with a VLT of

48%. Shading configuration S1 (unshaded) resulted in the highest value of DGP at 50.48% (intolerable), with a reduction in the glare value to 27.65% with an opaque overhang (S2).

Table 4. Tabulated results of the Guardian SunGuard HP Bronze 40/27 IGU static glass sample.

Test ID [Shading State]	Configuration	DGP [%]	DGP Classification	Number of Light Sources Identified	Luminance Threshold [cd/m^2]
S1	Unshaded	50.48	intolerable	44	3000
S2	Shaded (opaque overhang)	27.65	imperceptible	9	3000
S3	PDLC overhang ON (transparent)	40.01	disturbing	28	3000
S4	PDLC overhang OFF (translucent)	33.21	imperceptible	8	3000
S5	SPD overhang ON (bleached)	29.26	imperceptible	13	3000
S6	SPD overhang OFF (tinted)	26.28	imperceptible	8	3000

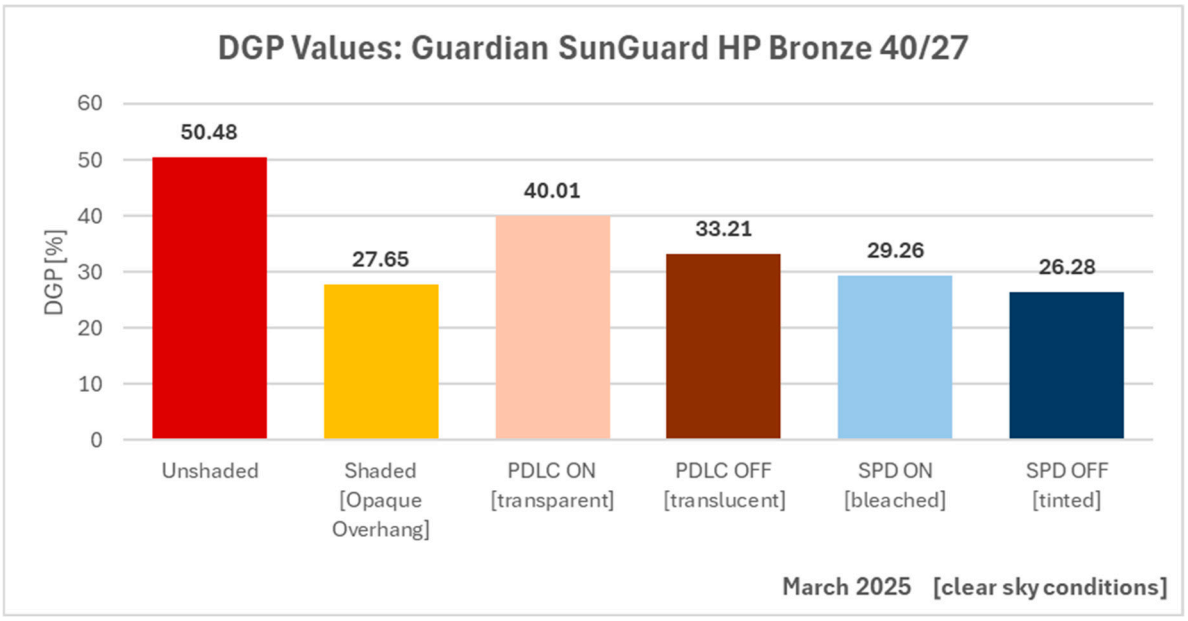

Figure 12. Graphical representation of the results of the Guardian SunGuard HP Bronce 0/27 static glass sample.

Comparing these benchmark readings to those achieved with the subsequent four shading configurations (S3–S6), one can observe that the PDLC overhang in its transparent state allows for a reduction of the glare value to 40.01%, marginally exceeding the perceptible limit on the DGP four-point scale classification. In its OFF (translucent) state, the DGP falls to 33.21%, again higher than that obtained with a fully opaque shading overhang. The SPD in its bleached state allows for a substantial reduction in the glare value to 29.26% (imperceptible). In its OFF (tinted) state, the DGP attained (26.28%) results in a slightly lower value than that obtained with the opaque shading overhang, again likely due to the white colour of the opaque overhang.

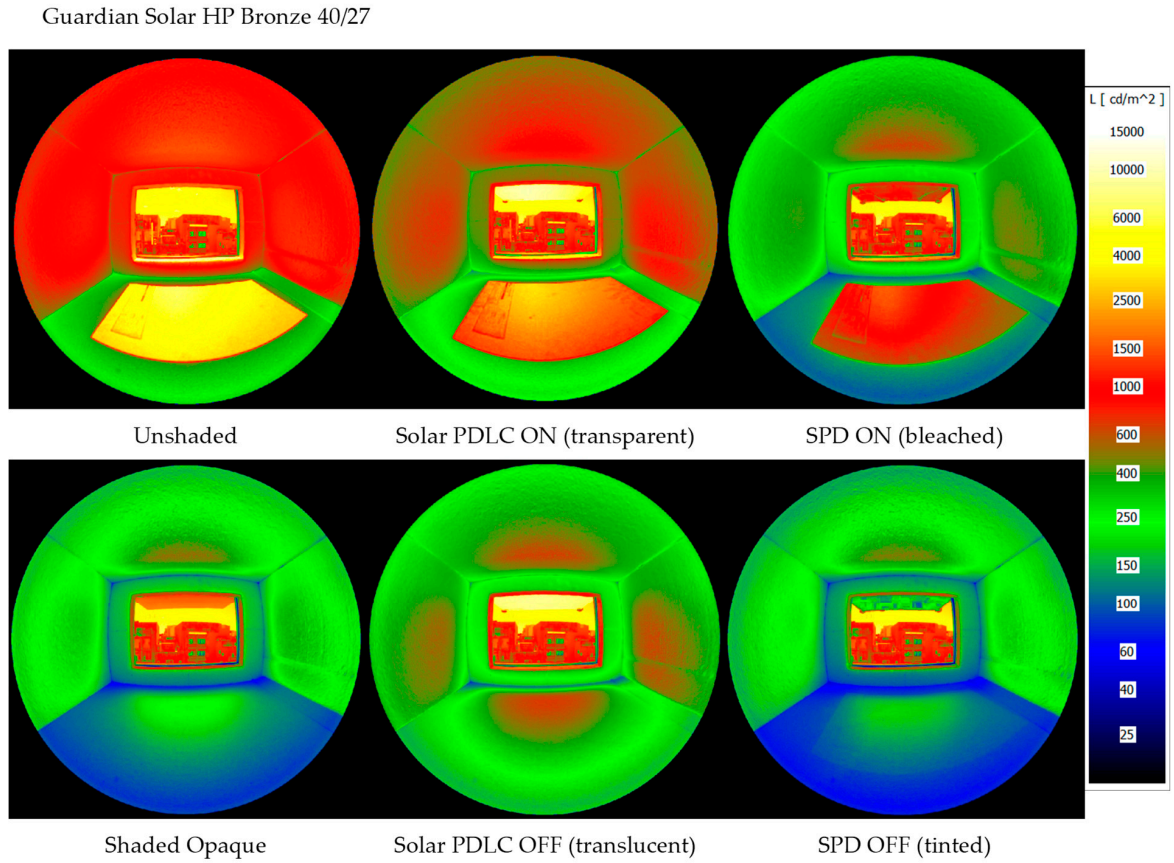

Figure 13. Luminance maps for the Guardian Solar HP Bronze 40/27 under different shading configurations.

3.3. Guardian Saint Gobain KN148 Static Glass Sample

Results obtained for the Saint Gobain KN148 static glass sample are as shown in Table 5 and Figures 14 and 15. The values of the DGP of the six shading configurations tested appear to correlate with the visible light transmittance of the sample under test. As expected, shading configuration S1 (unshaded) resulted in the highest value of DGP at 56.24% (intolerable) with a reduction in the glare value to 29.62% with an opaque overhang. Comparing these benchmark readings to those achieved with the subsequent four shading configurations (S3–S6), one can observe that the PDLC overhang in its transparent state allows for a reduction in the glare value to 45.46%, just above the disturbing bracket on the DGP four-point scale classification. In its OFF (translucent) state, the DGP falls on the lower end of the perceptible scale, which is higher than the value obtained with the opaque shading overhang. The SPD overhang in its bleached state allows for a further reduction in the glare value to 32.27% (imperceptible). In its OFF (tinted) state, the DGP attained 28.23%, which again is a lower value than that obtained with the opaque shading overhang.

Table 5. Tabulated results of the Saint Gobain KN148 static glass sample.

Test ID [Shading State]	Configuration	DGP [%]	DGP Classification	Number of Light Sources Identified	Luminance Threshold [cd/m^2]
S1	Unshaded	56.24	intolerable	9	3000
S2	Shaded (opaque overhang)	29.62	imperceptible	19	3000
S3	PDLC overhang ON (transparent)	45.46	intolerable	169	3000
S4	PDLC overhang OFF (translucent)	36.65	perceptible	20	3000
S5	SPD overhang ON (bleached)	32.37	imperceptible	34	3000
S6	SPD overhang OFF (tinted)	28.23	imperceptible	12	3000

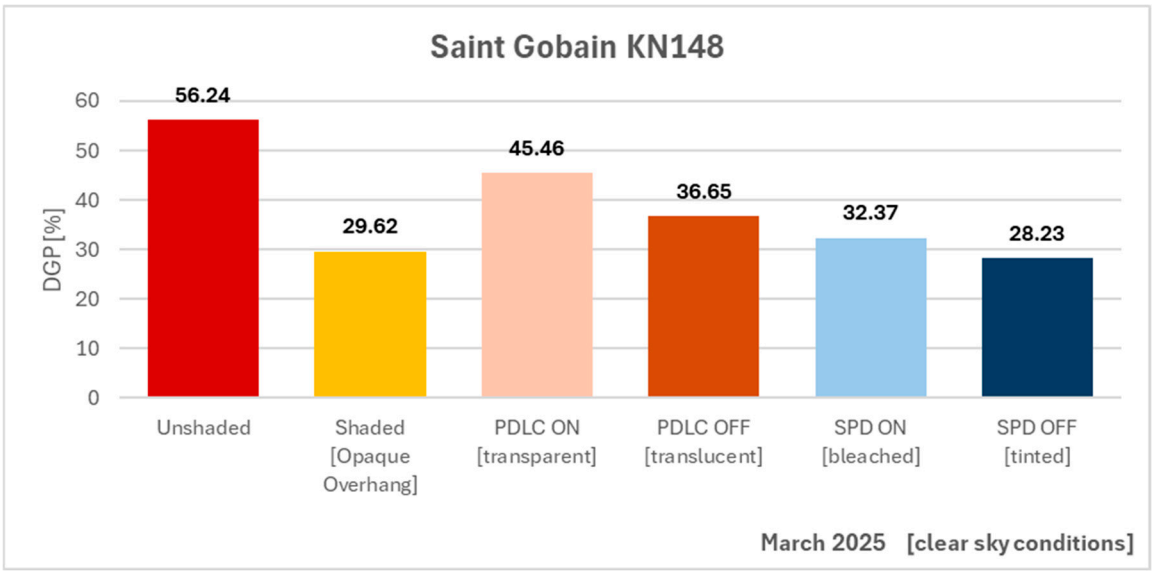

Figure 14. Graphical representation of the results of the Saint Gobain KN148 static glass sample.

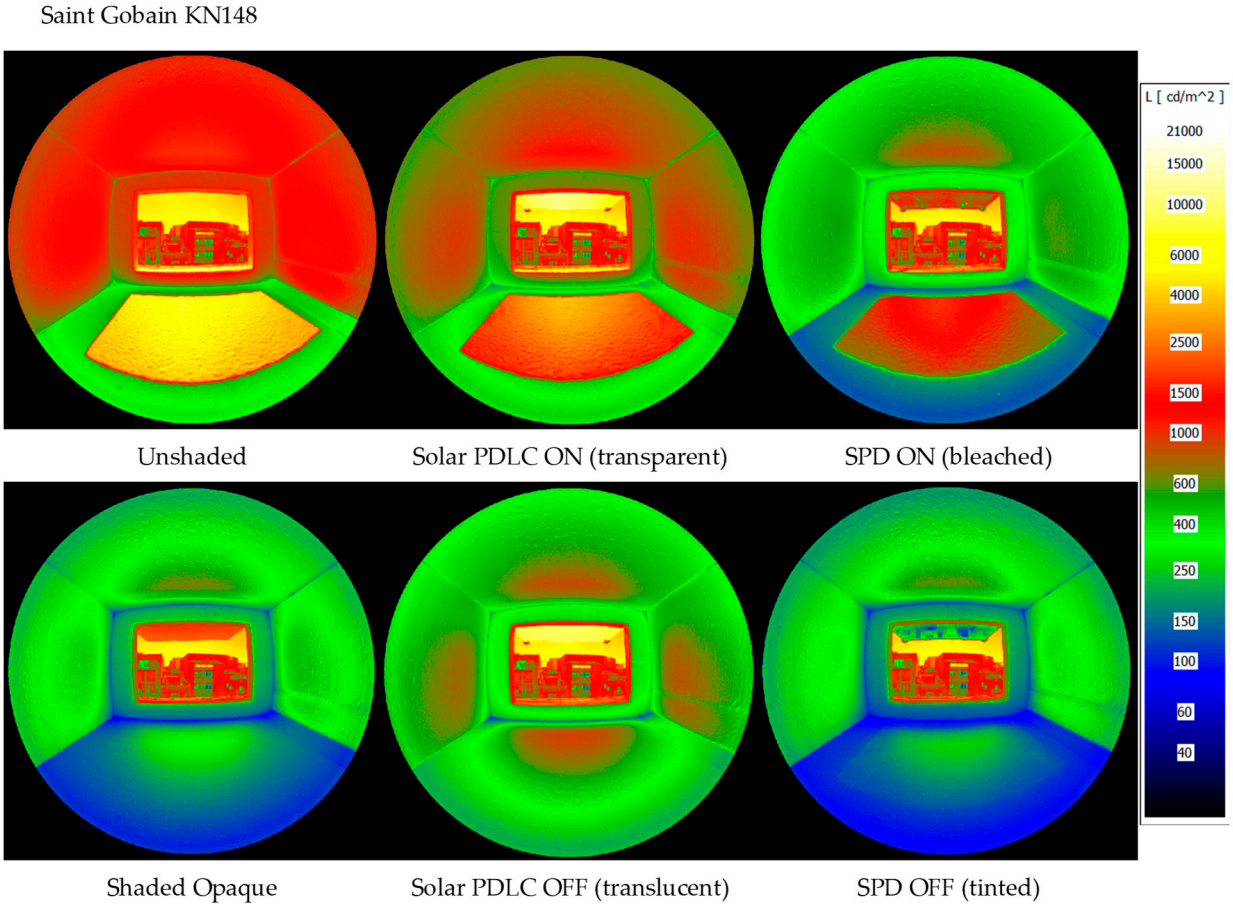

Figure 15. Luminance maps for the Saint Gobain KN148 under different shading configurations.

4. Discussion

This study is intended as an initial performance assessment for a possible novel application for switchable glazing. While real-world, full-scale testing is the ultimate benchmark for building integration, such studies often introduce environmental 'noise' that can obscure the direct optical relationship between dynamic glazing and visual comfort. By utilizing a controlled 1:10 scale model environment, this research isolates the transmittance-

driven performance of switchable shading. The findings serve as a critical proof of concept, providing the empirical evidence required to justify full-scale architectural testing while offering a validated dataset for future computational modelling.

4.1. VLT-DGP Correlation

A regression analysis for the unshaded static glass samples revealed a strong linear relationship between visible light transmittance (VLT) and Daylight Glare Probability (DGP) ($R^2 \approx 0.999$). This suggests that within the parameters of this study, VLT serves as a very strong predictor of the perception of glare (Figure 16).

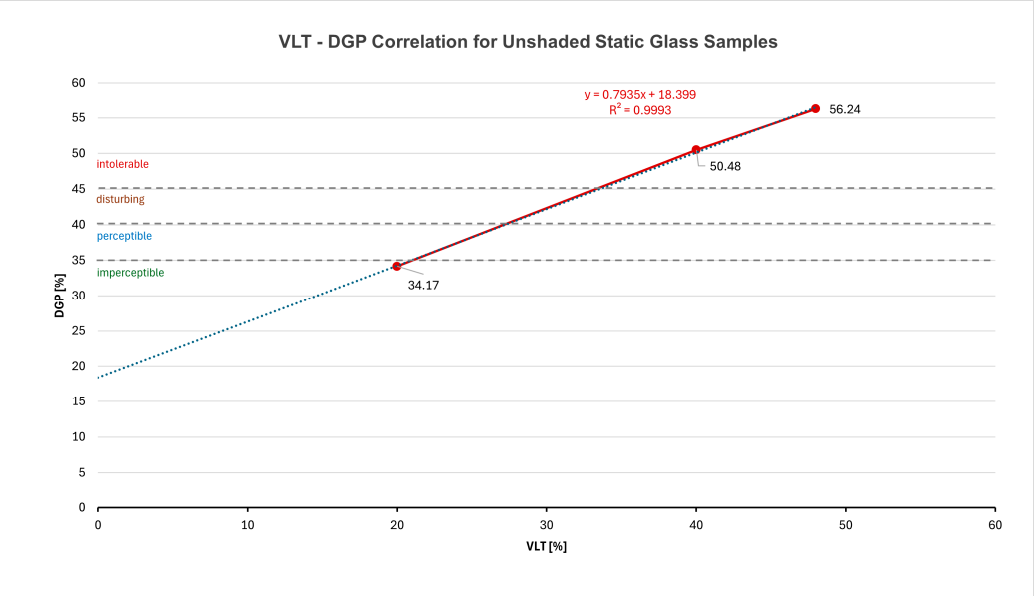

Figure 16. Plot showing the relationship between the VLT of the glass samples and the DGP (unshaded state).

While the sample size was limited to three glass types (N = 3), the result achieved a significance F (*p*-value) of 0.019, which satisfies the standard 95% confidence interval ($p < 0.05$). In the context of small-sample statistics, such a low *p*-value is only possible when the effect size is substantial and the data points align with precision. The high R^2 value likely reflects a fundamental physical consistency since DGP is a function of vertical illuminance and luminance, both of which are directly attenuated by the glass's transmittance. The relationship thus follows a predictable, linear path of light reduction. Despite these results, the following constraints must be acknowledged. With only one degree of freedom (df = N − 2 =1), the model is highly sensitive to measurement error since a single outlier would significantly alter the correlation. In addition, these results are strictly applicable to the tested range of VLT. These results ought to be considered as a strong indicator of correlation rather than an absolute rule.

Two similar regressions were also computed to assess the VLT-DGP relationships with the different switching states of the switchable shades. When comparing the unshaded state of the model with that featuring the PDLC-ON (transparent) and SPD-ON (bleached) states of the switchable overhangs, three linear relationships could be observed (Figure 17).

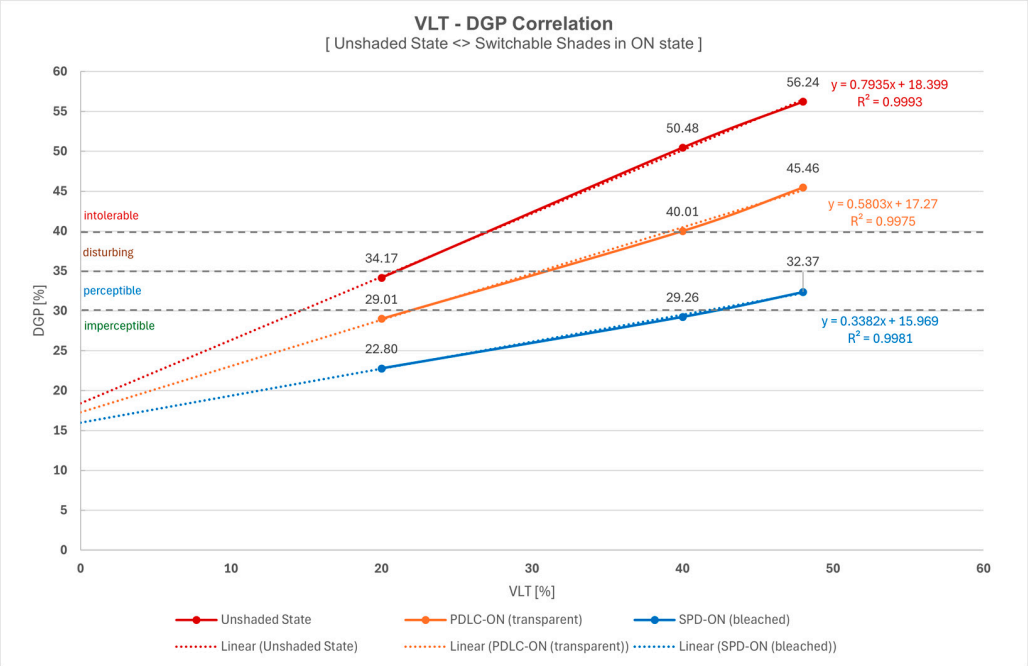

Figure 17. Plot showing the VLT-DGP correlation (unshaded <> PDLC-ON <> SPD-ON).

These plots demonstrate that the DGP results for the unshaded state, PDLC-ON (transparent) shade, and SPD-ON (bleached) shade are all correlated with the VLT of the static glass samples representing the glazed façade (20%, 40% and 48% VLT), with R^2 values of 0.9993, 0.9975, and 0.9981, respectively. In addition, all three linear relationships were also noted to correlate with the respective VLT (unshaded = 100% VLT; PDLC-ON = 72% VLT; SPD-ON = 45% VLT) of the switchable shades themselves. The unshaded state resulted in the topmost linear relationship with the steepest gradient (m = 0.7935). The PDLC shade in its ON state at 72% VLT yielded the middle linear relationship, with a slightly lower gradient (m = 0.5803). The SPD shade in its ON state at 45% VLT resulted in the lowermost linear relationship, with the shallowest gradient (m = 0.3382). These results further demonstrate that a constant reduction in the VLT of the switchable shades (100% − 72% = 28%; 72% − 45% = 27%) resulted in an approximately equal reduction in the gradient of each linear relationship (0.7935 − 0.5803 = 0.2132; 0.5803 − 0.3382 = 0.2421). It can thus be shown that both switchable shades in their ON (transparent / bleached) states generally lower the perception of glare when compared to the unshaded state, with the resultant relationship to the four classes of the DGP scale clearly dependent on the visible light transmittance of the window. From a visual perspective, a switchable glazed overhang in its ON state appears to have the potential of 'filtering' excessive impinging daylighting into a space. It still, however, allows for the formation of solar patch which is not too 'visually intense' to an occupant directly facing the window, thus giving a lower perception of glare.

A similar analysis has been carried out to compare the performance of the switchable shades in their OFF state when compared to the opaque overhang shaded state (Figure 18). A similar correlation between the DGP and the VLT of the glass samples representing the glazed façade has been shown, with R2 values of 0.9978 (opaque overhang), 0.9986 (PDLC-OFF), and 0.9994 (SPD-OFF), respectively. For these states, the solar–PDLC shade in its OFF state provided for highest DGP values demonstrated by the topmost linear relationship in Figure 18. This can be explained by the effect of light dispersion through the solar–PDLC film in its OFF state, together with the reflection of light into the model from the specular surface of the switchable shade itself. The opaque overhang and the SPD shade

in its OFF state, with both their VLT being 0, provided two similar linear relationships with a similar gradient (m = 0.2941; 0.267) and both within the 'imperceptible' class. While showing that all three linear relationships correlate with the respective VLT of the shades themselves, it can be shown that the SPD shade in its OFF state has the potential to provide for the same perception of glare as a conventional opaque overhang.

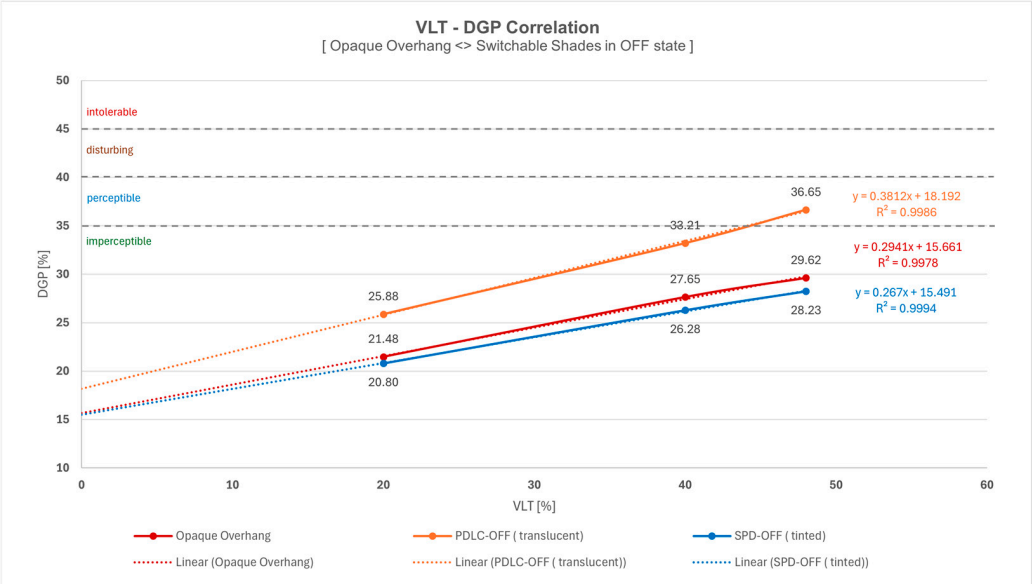

Figure 18. Plot showing the VLT-DGP correlation (opaque overhang <> PDLC-OFF <> SPD-OFF).

Cognisant of the fact that a limited sample size (n = 1 per strategy) precludes a formal *t*-test for statistical significance, these results can be evaluated against the known precision of the methodology. The instrumentation used has a resolution of 0.01% for the DGP calculations and maintains a Coefficient of Variance (CV) of 0.0066 in the case of scenes with high DGP values (greater than 0.70) and 0.0033 in the case of scenes with a low DGP (less than 0.27). This therefore indicates a high degree of repeatability. The smallest measured difference between any two shading strategies (Guardian Solar Bronze 20: opaque overhang vs. SPD OFF) is 0.68%, which exceeds 0.33% of the established noise base of the measurement system in the case of scenes with low DGP values. This suggests that even this small difference is a result of the shading performance rather than instrumental error. However, given these results, a larger sample size would be required to confirm statistical significance, as suggested in Section "Limitations and Future Work section".

4.2. Comparative Analysis

A comparative analysis was conducted for the test results attained for the March test run to better assess the performance of different shading configurations, with the results plotted in histograms (Figures 19–21). Three comparative analyses were considered appropriate:

- The magnitude of the DGP range between unshaded and shaded states;
- The differences in DGP between unshaded and shaded states in real terms;
- The percentage differences in DGP between unshaded and shaded states.

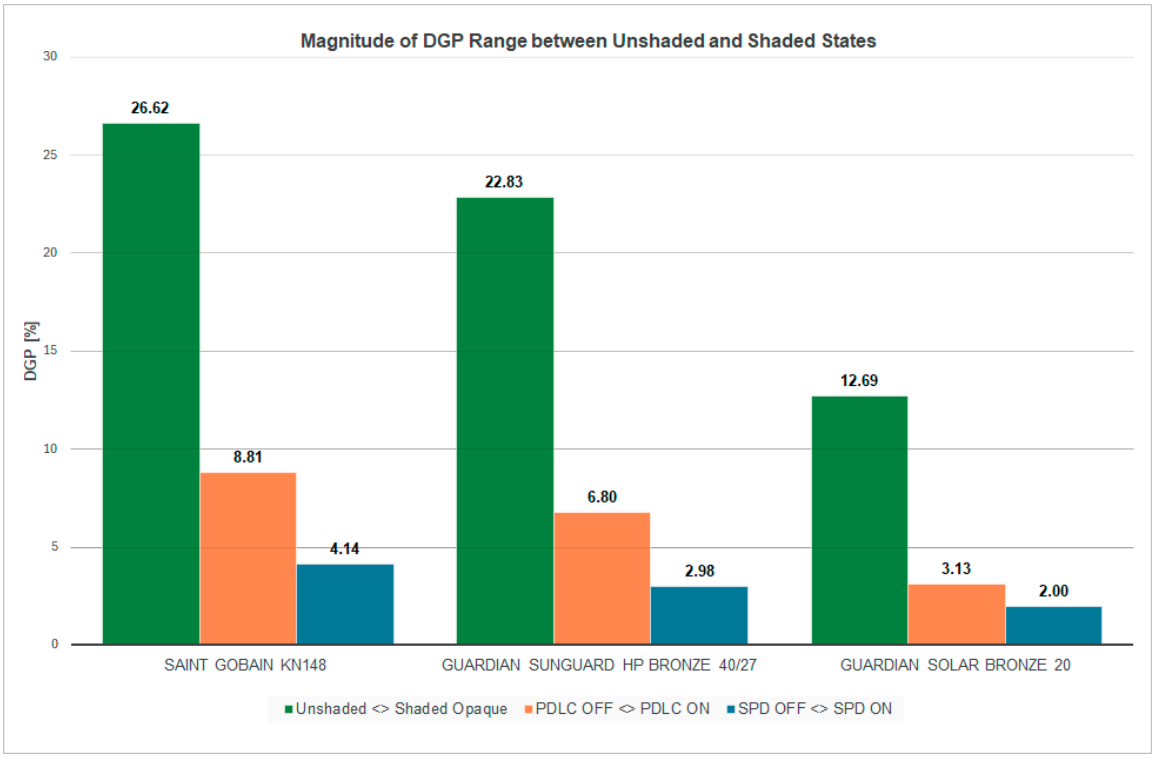

Figure 19. Graphical representation of the DGP range between unshaded and shaded states.

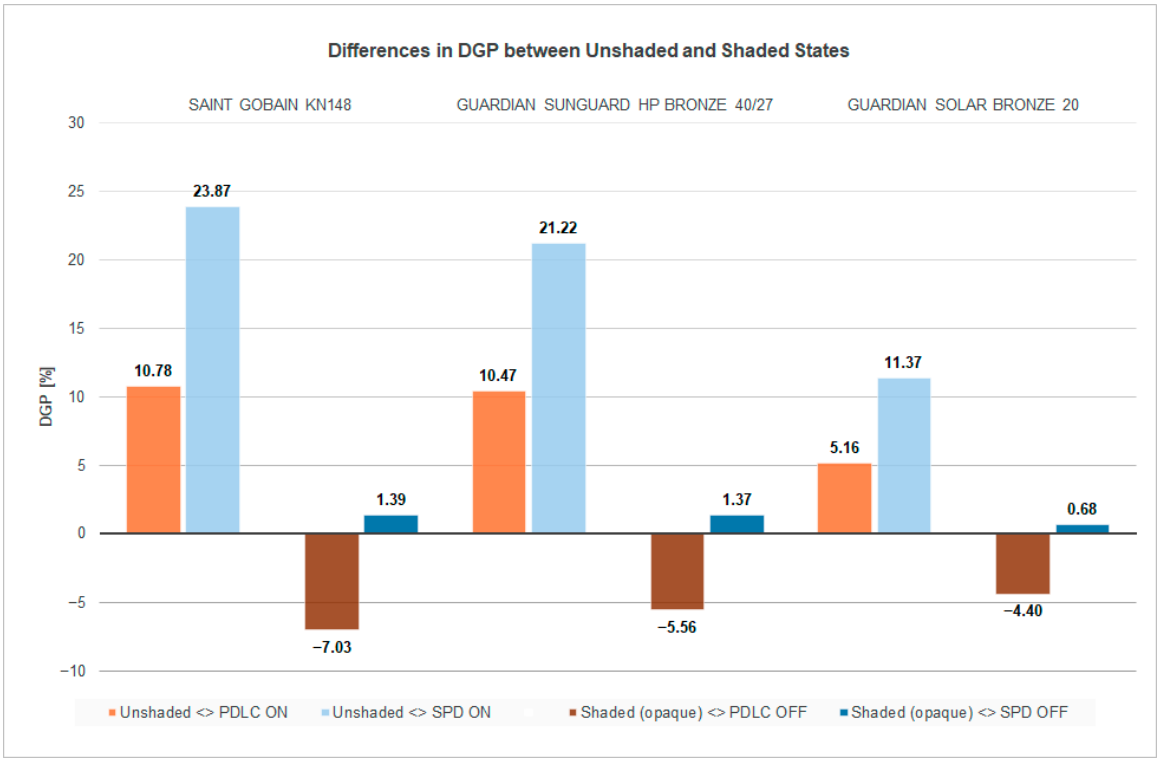

Figure 20. Graphical representation of the DGP differences in real terms between unshaded and shaded states.

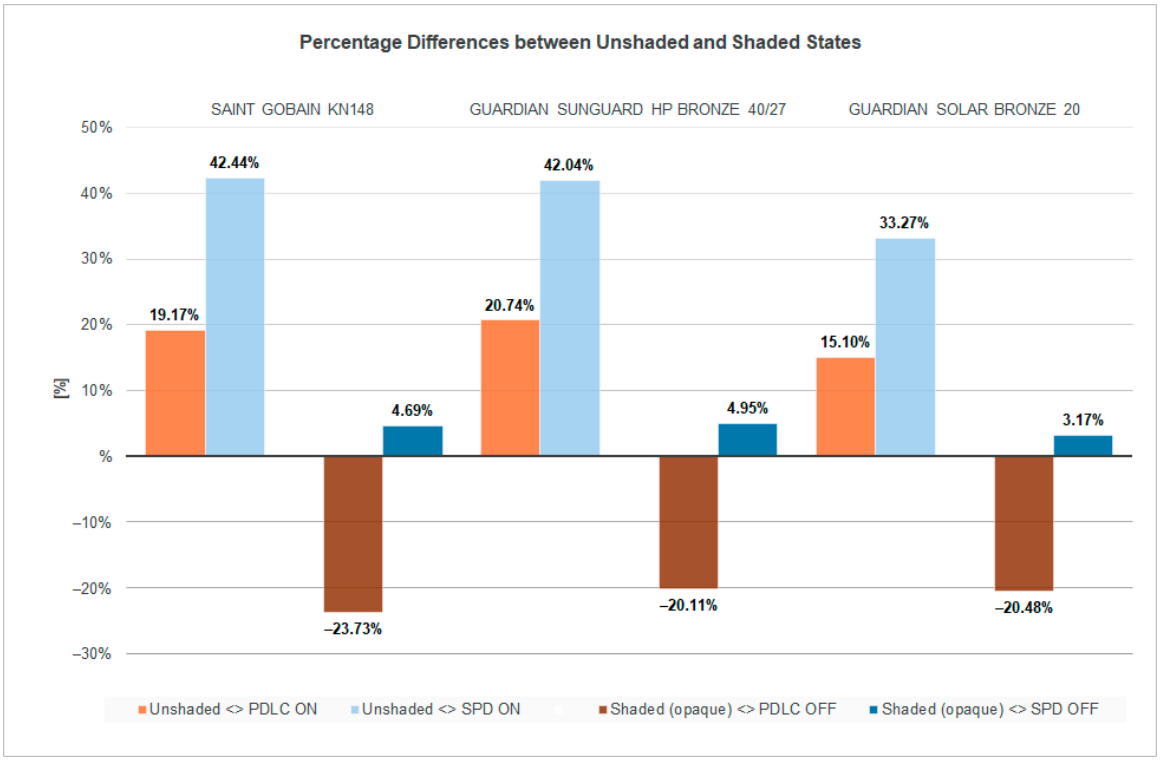

Figure 21. Graphical representation of the percentage DGP differences between unshaded and shaded states.

Figure 19 shows the difference in computed DGP values between the unshaded and shaded states of all shading combinations for the three static glass samples under consideration. Then results show that the values measured correlate with the visible light transmittance of the samples, with the Saint Gobain KN148 having the largest DGP values out of the three samples. The differences in DGP values between the completely unshaded and the shaded state (opaque overhang) are at absolute maximum for all three test samples, mainly due to the ability of the opaque shading overhang to completely block visible light through the material of shade itself.

The differences in DGP values of the switchable solar–PDLC overhangs were approximately 67%, 70%, and 75% less than the [unshaded <> shaded opaque] DGP difference for the Saint Gobain KN148, the Guardian SunGuard HP Bronze 40/27, and the Guardian Solar Bronze 20 samples, respectively. This shows that in its ON (transparent) state, a solar PDLC shade is still capable of blocking part of the incoming solar radiation due to the thickness of the glass laminate itself (9.62 mm) and the material properties of the PDLC film (parallel light transmittance in its ON state = 72%). With the solar rays hitting at an angle of 47° on the horizontal surface of the glass overhang, an element of light refraction through the glass together with partial dispersion of light caused by the PDLC film was noted to allow for a less glaring solar patch on the model's flooring. In its OFF (translucent) state, the shade was effective at blocking incoming solar radiation, as could be confirmed by the complete absence of a solar patch on the model's floor. The measured DGP value, slightly higher than that obtained with the shaded (opaque) configuration, is likely due to specular reflections from the surface of the glass overhang allowing for a slight increase in the penetration of light inside the model.

The differences in the DGP values of the switchable SPD overhangs were approximately 84%, 87%, and 84% less than the [unshaded <> shaded opaque] DGP differences for the Saint Gobain KN148, the Guardian SunGuard HP Bronze 40/27, and the Guardian Solar Bronze 20 samples, respectively. This shows that in its ON (bleached) state, an SPD

shade still allows for the shielding of part of the incoming solar radiation due to the thickness of the glass itself (9.5 mm) and the material properties of the SPD film (parallel light transmittance in its ON state = 45%). In its OFF (tinted) state, an SPD shade was noted to be as effective at blocking incoming solar radiation as a completely opaque shading overhang, possibly due to the dark blue colour of the SPD film itself. In this case, again, the complete absence of a solar patch on the model's floor could be visually observed.

Figures 20 and 21 show a comparison of the difference in computed DGP values (and in relative percentage) between the unshaded and shaded (opaque) overhang, here considered benchmarks, and each state of the switchable shading overhangs. The smaller the difference, the closer the performance of each state of the switchable shade to the respective benchmark. The results again show that the differences measured correlate with the visible light transmittance of the samples.

In the case of the solar PDLC switchable shade, the differences in DGP values between the unshaded benchmark and its ON (transparent) state featured a percentage decrease of 19.17%; 20.74% and 15.1%, respectively, in DGP readings for each of the three static glazing methods under consideration. These results show the extent to which this switchable shade can still offer a degree of solar protection, even in its transparent state. The results also show that the difference tends to decrease with the lesser visible light transmittance of the static glass installed on the façade.

The results of the SPD switchable shade in its ON (bleached) state show a larger difference in computed DGP values when compared to the unshaded benchmark configuration. Values show a percentage difference of 42.44%, 42.04%, and 33.37%, respectively, for each of the three static glazing methods under consideration. These results correlate with the visible light transmission of the static glass samples (48%, 40%, and 20% VLT, respectively) and confirm that in a horizontal configuration on a south-facing orientation, an SPD shade in its fully bleached state can effectively lower the level of indoor glare while still allowing for a solar patch to penetrate an indoor space. Moreover, in the case of the lowest visible light transmittance of the three static samples, the difference in DGP from the shaded opaque benchmark remains greater than that of the solar–PDLC shade.

Results for the OFF (translucent) states of the solar PDLC shade show a higher DGP value when compared to the shaded (opaque) benchmark configuration for all three static glass samples. These indicators show that in that state, the shade cannot lower the indoor glare rating to the same extent as that achieved by the opaque shade, showing a difference of 23.73%, 20.11%, and 20.48%, respectively, in computed glare value for each of the three static glazing methods under consideration. Although reflections by the specular surface of the glass of the switchable shade itself may be a contributing factor, the light dispersion properties of the PDLC film itself and its VLT of 72% in its OFF state are likely the reason for these results.

In their OFF (tinted) states, the SPD shade produces results very close to the DGP values given by the shaded (opaque) benchmark configuration for all three static glass samples. These indicators show that in that state, the shade is capable of lowering the indoor glare rating to almost the same extent as that achieved by the opaque shade, with a difference of only 4.69%, 4.95%, and 3.17%, respectively, in computed glare value for each of the three static glazing methods under consideration. When comparing these results to those computed with the solar–PDLC shade in its OFF (translucent) state, one can deduce that the effect of reflections by the specular surface of the glass of the switchable shade itself are likely to be offset by the material properties of the SPD film itself, particularly its lower albedo.

5. Conclusions

This paper investigates a novel application of two market-ready switchable glazing interlayers, solar-polymer-dispersed liquid crystal (PDLC) and suspended particle (SPD) switchable films, which are currently used as interlayers in architectural, automotive, and aviation glazing applications. The novel application is a switchable shading device which can be installed as an external horizontal overhang (in the case of a south-facing façade) directly above a glazed façade with conventional static glazing. Such an application would be equally suitable for new buildings and for retrofitting existing ones. On east and west-facing facades, its application as a shading device in a vertical orientation is expected to perform equally effectively. Two prototypes were considered: a solar–PDLC and an SPD shade. Using a scale model approach with a high glazing ratio representative of an office setup, field tests were conducted to assess and compare the indoor daylight conditions achieved using these shades when compared to those achieved by a conventional opaque static overhang. With tests carried out in March, a research-grade luminance photometer was used to capture a series of HDR images, from which luminance maps could be generated. The computation of the Daylight Glare Probability (DGP) for each scene was used as the comparative metric to assess the level of indoor glare representative of a building occupant seated at a distance and facing the window. Field test results show that even with a scale model, there is a remarkable difference in the value of the DGP for the same scene under different sky conditions and different sun altitudes. The size, brightness and penetration depth of the solar patch into an indoor space all have a bearing on the perception of glare. Moreover, the albedo and texture of indoor finishes have a substantial bearing on the level of the DGP, as does the visible light transmittance (VLT) of the static window glazing.

The results show that in the case of the three static samples in their unshaded state, there is a strong correlation between the visible light transmittance and the computed daylight glare probability, confirming that the VLT serves as a very strong predictor of the perception of glare. In both their ON (transparent/bleached) and OFF (translucent/tinted) states, the DGP attained by the switchable shades also correlated with the VLT of the static glass samples. In addition, the results also show that the difference in the VLT of the switchable shades themselves correlated with a reduction in the gradient of their respective VLT-DGP relationships in the case of their ON (transparent/bleached) state.

The difference in DGP readings between the unshaded configuration and those obtained with a conventional, horizontal overhang shade are at the highest and can thus be considered as being the upper and lower limits of the values obtained in these experiments. The prototype solar–PDLC and SPD shades both show promising visual performance in that they both can effectively allow or restrict the formation of a solar patch within an indoor space dynamically. The solar–PDLC switchable shade was demonstrated to perform better than the SPD film in achieving visual transparency when the building occupant would want to allow for the sun to come into an indoor space. Both the colour tone of the film and its material properties appear to perform this function better while still shielding excessive daylighting that would otherwise have resulted without any form of shading being deployed. The SPD film was observed to allow for a visually more subtle solar patch, which can still be desirable for a building occupant in certain circumstances.

In their OFF (translucent/tinted) states, both solar–PDLC and SPD switchable shades demonstrated very good performance in block incoming solar radiation, thus providing shade. The solar–PDLC laminate allowed for a higher DGP that that computed with an opaque shade, meaning that both specular reflections from the glass surface of the shade itself and the material properties of the film in the form of light dispersion provided for a slight increase in DGP, albeit within acceptable limits for static window glazing of 40% or

less. The switchable SPD film, on the other hand, performed better in its OFF (tinted) state in that it allowed for DGP values close to those achieved with a static (opaque) overhang.

Besides this initial analysis of the DGP performance of the switchable shades under study, this paper identifies the potential psychological advantages of having these technologies deployed as shading devices. Although DGP metrics show a narrower range of values between the unshaded and shaded states of films, when compared to the wider range of values between unshaded and shaded (opaque) configurations, the possibility of allowing a building occupant to have control over the transparency of a shading overhang to control the level of daylight without resorting to indoor blinds is a benefit that surely merits further consideration. This study thus shows that this novel application has the potential to control glare without compromising views while providing adaptable external shading without any mechanical and moving parts. In addition, the degree of solar protection offered by both switchable shades even in their transparent state is a property that merits further study in that a desirable solar patch can still be allowed into the building, particularly in winter months, which would otherwise not be possible with a fixed opaque shading overhang. The prospect of retrofitting applications of such technologies is also worth mentioning. It can be demonstrated that through the limited intervention of installing such dynamic shading devices on existing facades with poor-performing glazing in terms of visual comfort, a static façade can be converted into a vibrant adaptable building envelope.

Limitations and Future Work

The findings presented in this paper show that the performance of the novel switchable shading device is promising and merits further detailed investigations. While the research design ensures high internal validity through strict temporal and geometric controls, certain limitations apply. The data represents a performance 'snapshot' under specific sky conditions. While the 60 minute window ensured stable sky luminance for comparison, it does not account for seasonal solar variations. Additionally, while 1:10 scale modelling is a validated analogue for daylighting studies due to the scale-independence of luminance, minor architectural details found in full-scale assemblies were simplified to focus on the core optical performance of the glazing.

Additional field test measurements using the same scale model under different solar angles of elevation, at times of day, and from different points of observation would provide additional performance data to further validate this concept. A possible improvement to the prototype would be the use of matte glass for the switchable shades to reduce specular reflections into the indoor space. Full-scale field tests are also required to validate the findings from the scale model and perform more detailed measurements. To this end, two full-scale mock office setups have been installed at the University of Malta campus (35°54′5″ N 14°28′79″ E) specifically to perform further experiments and investigations. Full-scale field tests of such switchable shades would provide additional data in a real-life setup for visual, thermal, and energy performance assessments. Moreover, occupant satisfaction tests with human participants are crucial in studies of this nature, particularly to assess the level of satisfaction or otherwise with having a switchable shading device fitted in an office environment The assessment of responses from human participants when given direct control of a "shadow on demand" provided by a switchable shading device is considered essential before drawing definitive conclusions in this field of research. Further research should also delve into the practical and technical aspects of assembly, installation, and detailing of such glazed shading devices in existing and new facades.

https://doi.org/10.3390/buildings16081519

Author Contributions: Conceptualization, E.M.; Methodology, E.M., V.B. and M.O.; Validation, E.M.; Formal analysis, E.M.; Investigation, E.M.; Resources, E.M., V.B. and M.O.; Data curation, E.M.; Writing—original draft, E.M.; Writing—review & editing, E.M. and V.B.; Visualization, E.M.; Supervision, V.B. and M.O.; Project administration, E.M. and V.B.; Funding acquisition, E.M. and V.B. All authors have read and agreed to the published version of the manuscript.

Funding: The authors acknowledge the co-financing provided by the Malta Government Endeavour (Group B) 3rd Call Scholarship Scheme 2017 (Grant No. MEDE/1117/2017/53).

Institutional Review Board Statement: Not applicable.

Data Availability Statement: The datasets presented in this article are not readily available since they form part of an ongoing study. Requests to access the datasets should be directed to etienne.magri.99@um.edu.mt.

Acknowledgments: The present work was developed within the framework of a PhD research project. The authors would like to thank the Department of Environmental Design at the University of Malta; the Department of Architectural Engineering at TU Delft; GAUZY Ltd.; Floatglass (Malta) Ltd.; and F. Schembri Holdings (Malta) Ltd. for the necessary collaboration.

Conflicts of Interest: The authors declare no conflicts of interest.

References

1. Ben Bacha, C.; Bourbia, F. Effect of kinetic facades on energy efficiency in office buildings—Hot dry climates. In Proceedings of the 11th Conference on Advanced Building Skins, Bern, Switzerland, 10–11 October 2016.
2. Dhayal, P.; Jha, B. Indoor Visual Comfort: A Review of Factors and Assessments. *Int. Soc. Study Vernac. Settl.* **2023**, *10*, 38–59. [CrossRef]
3. *BS EN 17037:2018*; Daylight in Buildings. The British Standards Institution, BSI Standards Ltd.: London, UK, 2019.
4. Ibrahim, I.; Nour, W.; Elwan, M. Visual privacy as an approach to improve human needs in residential buildings in Egypt. *J. Eng. Res.* **2023**, *7*, 13.
5. Magri, E.; Buhagiar, V.; Overend, M. Field assessment of visual performance of a dynamic dual glazing assembly for occupants with lateral incident light. *J. Phys. Conf. Ser.* **2025**, *3140*, 102004. [CrossRef]
6. Ghosh, A.; Norton, B. Advances in switchable and highly insulated autonomous (self-powered) glazing systems for adaptive low energy buildings. *Renew. Energy* **2018**, *126*, 1003–1031. [CrossRef]
7. Ghosh, A.; Norton, B.; Duffy, A. Behaviour of a SPD switchable glazing in an outdoor test cell with heat removal under varying weather conditions. *Appl. Energy* **2016**, *180*, 695–706. [CrossRef]
8. Ghosh, A.; Norton, B.; Duffy, A. Measured overall heat transfer coefficient of a suspended particle device switchable glazing. *Appl. Energy* **2015**, *159*, 362–369. [CrossRef]
9. Bodart, M.; Cauwerts, C. Assessing daylight luminance values and daylight glare probability in scale models. *Build. Environ.* **2017**, *113*, 210–219. [CrossRef]
10. Yngvesson, L.; Adolfsson, E. The Impact of Scale When Using Models of Daylight Analysis. Bachelor's Thesis, Jönköping Technical University, Jönköping, Sweden, 2018.
11. Hopkinson, R.G. Glare from daylighting in buildings. *Appl. Ergon.* **1972**, *3*, 206–215. [CrossRef] [PubMed]
12. Iwata, T.; Shukuya, M.; Somekawa, N.; Kimura, K.-I. Experimental study on discomfort glare caused by windows—Part 1: Subjective Response to glare from a simulated window. *J. Arch. Plan. Environ. Eng. (Trans. AIJ)* **1992**, *432*, 21–33. [CrossRef]
13. Iwata, T.; Tokura, M.; Shukuya, M.; Kimura, K.-I. Experimental study on discomfort glare caused by windows—Part 2: Subjective response to glare from actual windows. *J. Arch. Plan. Environ. Eng. (Trans. AIJ)* **1992**, *439*, 19–31. [CrossRef]
14. Waters, C.E.; Mistrick, R.G.; Bernecker, C.A. Discomfort Glare from Sources of Nonuniform Luminance. *J. Illum. Eng. Soc.* **1995**, *24*, 73–85. [CrossRef]
15. Velds, M. Assessment of Lighting Quality in Office Rooms with Daylighting Systems. Ph.D. Thesis, Delft University of Technology, Delft, The Netherlands, 1999.
16. Wienold, J.; Christoffersen, J. Evaluation methods and development of a new glare prediction model for daylight environments with the use of CCD cameras. *Energy Build.* **2006**, *38*, 743–757. [CrossRef]
17. Matin, N.H.; Eydgahi, A.; Gharipour, A. Sustainable Design: Minimizing Discomfort Glare Through Data-Driven Methods for Responsive Facades. *Sustainability* **2025**, *17*, 783. [CrossRef]
18. Pierson, C.; Cauwerts, C.; Bodart, M.; Wienold, J. Tutorial: Luminance Maps for Daylighting Studies from High Dynamic Range Photography. *Leukos* **2021**, *17*, 140–169. [CrossRef]

19. Pierson, C.; Wienold, J.; Bodart, M. Daylight Discomfort Glare Evaluation with Evalglare: Influence of Parameters and Methods on the Accuracy of Discomfort Glare Prediction. *Buildings* **2018**, *8*, 94. [CrossRef]
20. Wienold, J. Dynamic Daylight Glare Evaluation. In Proceedings of the International Building Performance Simulation Association, Glasgow, Scotland, 27–30 July 2009; pp. 944–951.
21. Reinhart, C.; Wienold, J. The daylighting dashboard—A simulation-based design analysis for daylit spaces. *Build. Environ.* **2011**, *46*, 386–396. [CrossRef]
22. Bian, Y.; Luo, T. Investigation of visual comfort metrics from subjective responses in China: A study in offices with daylight. *Build. Environ.* **2017**, *123*, 661–671. [CrossRef]
23. Wienold, J.; Christoffersen, J. Towards a New Daylight Glare Rating. In Proceedings of the 10th European Lighting Conference, Lux Europa 2005, Berlin, Germany, 19–21 September 2005.
24. Ruck, N.; Aschehoug, O.; Aydinli, S.; Christofferesen, J.; Courret, G.; Edmonds, I.; Jakobiak, R.; Kischoweit-Lopin, M.; Klinger, M.; Lee, E.; et al. *Daylight in Buildings: A Source Book on Daylighting Systems and Components*; International Energy Agency (IEA): Paris, France; Lawrence Berkeley National Laboratory (LBLN): Berkeley, CA, USA, 2000.